



The Inflammatory Effects of Dietary Lipids Regulate Growth of Parasites during Visceral Leishmaniasis

Ellen T. Kiser,^a Mark A. Wacker,^{b*} Upasna Gaur Dixit,^b Hemali Batra-Sharma,^{c*} Yani Chen,^{b,d}  Mary E. Wilson^{a,b,c,d}

^aDepartment of Microbiology and Immunology, Carver College of Medicine, University of Iowa, Iowa City, Iowa, USA

^bDepartment of Internal Medicine, Carver College of Medicine, University of Iowa, Iowa City, Iowa, USA

^cCarver College of Medicine, University of Iowa, Iowa City, Iowa, USA

^dVeterans' Affairs Medical Center, Iowa City, Iowa, USA

Ellen T. Kiser and Mark A. Wacker contributed equally to this work; E.T.K. generated the large data analyses and figures and so is listed first.

ABSTRACT Visceral leishmaniasis is a potentially fatal disease caused by the protozoan *Leishmania donovani* or *L. infantum* (Li). Although previous studies revealed that high lipid intake reduces parasite burdens in *Leishmania donovani*-infected mice, the specific contributions of dietary lipids to Li-associated pathogenesis are not known. To address this, we evaluated parasite growth, liver pathology, and transcriptomic signatures in Li-infected BALB/c mice fed either a control, high-fat, high-cholesterol, or high-fat-high-cholesterol diet. Using quantitative PCR (qPCR), we observed significantly reduced liver parasite burdens in mice fed the high-fat-high-cholesterol diet compared to mice fed the control diet. In contrast to the liver, parasite expansion occurred earlier in the spleens of mice fed the experimental diets. Histological examination revealed an intense inflammatory cell infiltrate in livers predominantly composed of neutrophils caused by the high-fat-high-cholesterol diet specifically. After 8 weeks of infection (12 weeks of diet), Illumina microarrays revealed significantly increased expression of transcripts belonging to immune- and angiogenesis-related pathways in livers of both uninfected and Li-infected mice fed the high-fat-high-cholesterol diet. These data suggest that increased fat and cholesterol intake prior to Li infection leads to a hepatic inflammatory environment and thus reduces the parasite burden in the liver. Defining inflammatory signatures as well as pathology in the liver may reveal opportunities to modify the therapeutic approach to Li infection.

IMPORTANCE Leishmaniasis is a spectrum of diseases caused by *Leishmania* species protozoa that is most common in warm climates, coinciding with impoverished regions. Visceral leishmaniasis is a potentially fatal disease in which parasites infect reticuloendothelial organs and cause progressive wasting and immunocompromise. The distribution and demographics of visceral leishmaniasis have changed over recent years, coinciding with modernizing societies and the increased availability of Western diets rich in lipid content. We report here that increased dietary fat and cholesterol intake affected disease pathogenesis by increasing inflammation and reducing localized parasite burdens in the liver. These diet-induced changes in disease pathogenesis might explain in part the changing epidemiology of visceral leishmaniasis. A relationship between diet and inflammatory responses may occur in leishmaniasis and other microbial or immune-mediated diseases, possibly revealing opportunities to modify the therapeutic approach to microbial infections.

KEYWORDS dietary lipids, inflammation, leishmaniasis, neglected tropical diseases, transcriptome

Citation Kiser ET, Wacker MA, Dixit UG, Batra-Sharma H, Chen Y, Wilson ME. 2021. The inflammatory effects of dietary lipids regulate growth of parasites during visceral leishmaniasis. *mSphere* 6:e00423-21. <https://doi.org/10.1128/mSphere.00423-21>.

Editor Ira J. Blader, University at Buffalo

This is a work of the U.S. Government and is not subject to copyright protection in the United States. Foreign copyrights may apply.

Address correspondence to Mary E. Wilson, mary-wilson@uiowa.edu.

* Present address: Mark A. Wacker, Department of Biology, Central Michigan University, Mt. Pleasant, Michigan, USA; Hemali Batra-Sharma, Department of Internal Medicine, University of California, San Diego, San Diego, California, USA.

 Diets high in fat and cholesterol affect the outcome of the parasitic infection leishmaniasis in mouse models.

Received 10 May 2021

Accepted 14 June 2021

Published 14 July 2021

Leishmaniasis, a vector-borne disease caused by *Leishmania* species parasites, leads to human morbidity or mortality in more than 100 countries (1, 2). Leishmaniasis refers to a spectrum of human diseases ranging from self-healing cutaneous leishmaniasis to visceral leishmaniasis (VL); the latter is the most severe form and causes most leishmaniasis-related fatalities (3). Clinical manifestations with different strains of each species of *Leishmania* can be highly variable, but the infecting species is a major determinant of the type of disease syndrome (3). VL is usually due to infection by *Leishmania infantum* (Li) or *Leishmania donovani* (4). Even after cure of symptomatic disease, parasites can be found in a quiescent state within host tissues of many, and possibly all, infected individuals (5, 6). It is not fully understood what host- or parasite-specific factors determine whether some patients remain asymptomatic whereas others develop severe VL, and these factors must be critically important determinants of the outcome of infection.

Sandflies, the insect vector of leishmaniasis, inoculate infectious parasites into the human dermis, after which the parasites are phagocytized by myeloid cells and can manipulate the host's immune response to their own survival advantage (4, 7–9). In addition to these perturbances of the immune response, individuals infected with *Leishmania* species parasites have characteristic changes in serum lipid profiles. More specifically, human patients with VL have elevated triglycerides and reduced cholesterol levels (10–12) as well as decreased levels of some apolipoproteins (13). Additionally, at least two transcriptional profiling studies highlight lipid metabolic pathways among the “most relevant” pathways modulated by *Leishmania* species infection of mouse bone marrow-derived macrophages (14, 15).

Rather than a unique mechanism incited by *Leishmania* species parasites, the above-described metabolic changes may reflect the changes in lipid metabolism occurring during many infectious diseases (11, 16). Although these changes are transient, they almost certainly affect immune responses to the infection. Indeed, one study reported that the parasite metalloprotease gp63 alters host microRNA 122 (miR-122), leading to lower serum cholesterol levels (17). Furthermore, the addition of exogenous host microRNA 122 during *L. donovani* infection led to the return of cholesterol to normal levels and a reduction of the parasite burden (17).

In regions of Brazil where *Leishmania* is endemic, increased prevalences of obesity and food insecurity reflect dietary changes (18, 19), and the effects of these dietary changes on the outcome of *Leishmania* infection have not been fully investigated. Ghosh et al. demonstrated that C57BL/6 mice fed a high-fat-high-cholesterol diet (21.1% fat and 1.3% cholesterol) prior to infection with *L. donovani* had significantly reduced parasite burdens in spleens and livers at 3 and 6 weeks postinfection, compared to mice fed a control diet (20). In contrast, another study showed that C57BL/6 mice fed a high-sugar and -butter diet had increased Li parasite burdens in their spleens and livers at 8 weeks postinfection (21). Parasite species and diet are possibly the explanation for these discrepancies. Nevertheless, we hypothesized that there might be more mechanisms underlying these divergent effects of elevated dietary lipids on the outcome of *Leishmania* infection.

Here, we investigated the effects of dietary manipulation of fat and cholesterol on the transcriptional profiles of mouse livers and the outcome of Li infection. Our data revealed not only changes in liver transcriptional profiles but also changes in parasite loads, which were divergent between the spleen and the liver. These data raised the possibility that transient manipulation of dietary intake during leishmaniasis might be advised as a synergistic approach with drug therapy in the management of leishmaniasis.

RESULTS

Diet alters the kinetics of parasite growth and histological response to Li infection. To explore the mechanisms by which dietary lipids influence the course and severity of VL, mice were maintained on a control diet or one of three experimental diets (high fat, high cholesterol, or high fat-high cholesterol) for 4 weeks prior to inoculation with Li or phosphate-buffered saline (PBS). The diets were continued for the

TABLE 1 Macronutrients and cholesterol in experimental diets^a

Diet component	% content (% kcal)			
	Control	High fat (TD.88137)	High cholesterol (TD.01383)	High fat-high cholesterol (TD.02028)
Protein	18.6	17.3 (15.2)	17.8 (22.9)	17.3 (15.5)
Carbohydrates	44.2	48.5 (42.7)	47.0 (60.5)	46.9 (41.9)
Fat	6.2	21.2 (42.0)	5.7 (16.6)	21.2 (42.6)
Cholesterol		0.2	2	1.3

^aDiets were obtained from Envigo (Indianapolis, IN). The percentages (by weight) of each macronutrient and cholesterol are listed. The percentages of kilocalories for macronutrients are also listed in parentheses for the experimental diets.

duration of the experiment. Macronutrient and cholesterol compositions of the diets can be found in Table 1. Eight weeks after inoculation (12 weeks on the diets), liver weights were significantly increased in both uninfected and infected mice fed the high-fat–high-cholesterol diet compared to mice fed the control diet. The spleen weight was also significantly increased in Li-infected mice after 12 weeks of the high-fat and the high-fat–high-cholesterol diets (Fig. 1A).

Murine leishmaniasis usually follows a pattern of the parasite burden peaking in livers after 4 to 6 weeks of infection; this is followed by resolution in the liver and a gradual increase of the parasite burden in the spleen (22, 23). Using quantitative PCR (qPCR), we observed that parasite burdens in the livers and spleens of Li-infected mice fed the control diet followed these expected kinetics (Fig. 1B). Parasite burdens in mice fed the experimental diets deviated significantly from the usual kinetics, and the changes were most exaggerated in mice fed the high-fat–high-cholesterol diet (Fig. 1B). Mice fed the high-fat–high-cholesterol diet had lower liver parasite burdens after 4 and 8 weeks of infection (also illustrated by an *in vitro* imaging system [IVIS] at 4 weeks) (Fig. 1C). In contrast, parasite loads in the spleens of mice fed the high-fat–high-cholesterol diet rose to significantly higher levels after 8 weeks of infection than in animals fed the control diets (Fig. 1B). Thus, a high-fat–high-cholesterol diet changed the organ-specific amplification of parasites during the first 2 months of infection, making the liver refractory and the spleen more susceptible.

The drastic decrease in liver parasite loads in the livers of mice fed the high-cholesterol–high-fat diet led us to investigate diet-induced changes in the liver environment of uninfected mice, the environment in which the parasites were introduced. Histological slides of livers were stained with hematoxylin and eosin (H&E) to determine cellular content and with Oil-Red-O to examine neutral lipids (Fig. 2). Microscopic enumeration of the H&E-stained slides revealed significant leukocytic infiltration, which was composed primarily of polymorphonuclear leukocytes (PMNs). For mice fed the high-fat–high-cholesterol diet, we observed significant increases in both lymphocytes and PMNs (Fig. 2A).

Oil-Red-O staining indicated that liver parenchymal cells, likely hepatocytes or stellate cells (24), of mice fed the experimental diets were enriched in lipid bodies compared to the livers of mice fed the control diet (Fig. 2B). The lipid bodies were substantially larger in mice fed the experimental diet than in mice fed the control diet, and the largest lipid bodies were observed in mice fed a high-fat diet. This suggested that there might be substantial changes in hepatocytes contributing to the altered liver environment prior to infection with Li.

A high-fat–high-cholesterol diet caused the most extreme transcript changes.

Total liver transcriptomes were sequenced to observe potential mechanisms underlying the shift in parasite growth kinetics in animals fed the experimental diets. RNA was extracted from the total liver homogenates of mice after 8 weeks of Li infection (12 weeks of the diets), as outlined in Table 1.

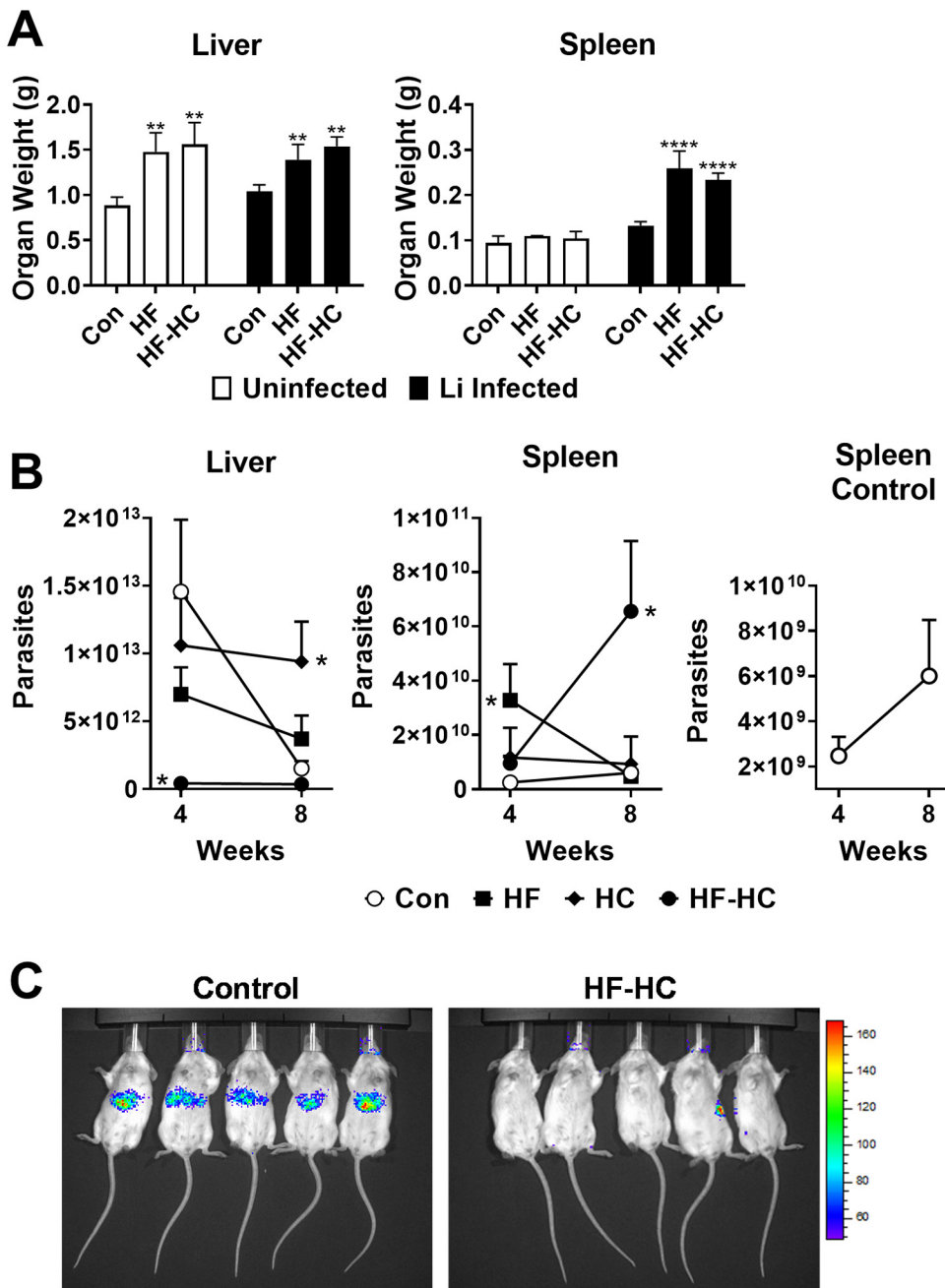


FIG 1 (A) Diet impacts organ weight. Organs were collected from Li-infected and uninfected BALB/c mice after 8 weeks of the experimental diets. The liver and spleen were weighed ($n = 2$ replicates for uninfected mice and 5 replicates for infected mice) (means and standard deviations) (**, $P < 0.005$; ****, $P < 0.0001$ [by two-way ANOVA with a Sidak posttest comparing uninfected and infected mice fed the experimental diets to uninfected mice fed the control {Con} diet]). HF, high fat; HF-HC, high fat-high cholesterol. (B) Diet changed infection kinetics. At 4 and 8 weeks postinfection, BALB/c mice were euthanized, and qPCR was performed using primers targeting Li kinetoplast DNA. For each mouse, two technical replicates were analyzed, and the mean was determined before calculating the number of parasites per liver and spleen using the comparative C_T method. The mean numbers of parasites per liver and spleen were then pooled, and outliers were removed before calculating the mean for each experimental group ($n = \sim 15$ [3 independent experiments with $n = \sim 5$ for each]; ROUT identified and removed ≤ 4 outliers per group) (means and standard errors of the means [SEM]) (*, $P < 0.05$ [by one-way ANOVA with a Dunnett posttest comparing experimental diets to the control diet]). (C) IVIS images reflect qPCR at 4 weeks. BALB/c mice fed experimental diets were infected with Li transfected to express the firefly luciferase gene, and infection status was monitored by IVIS. Parasite localization was imaged 10 and 15 min after luciferin administration. Images were taken at 4 weeks postinfection. The key indicates the number of pixels.

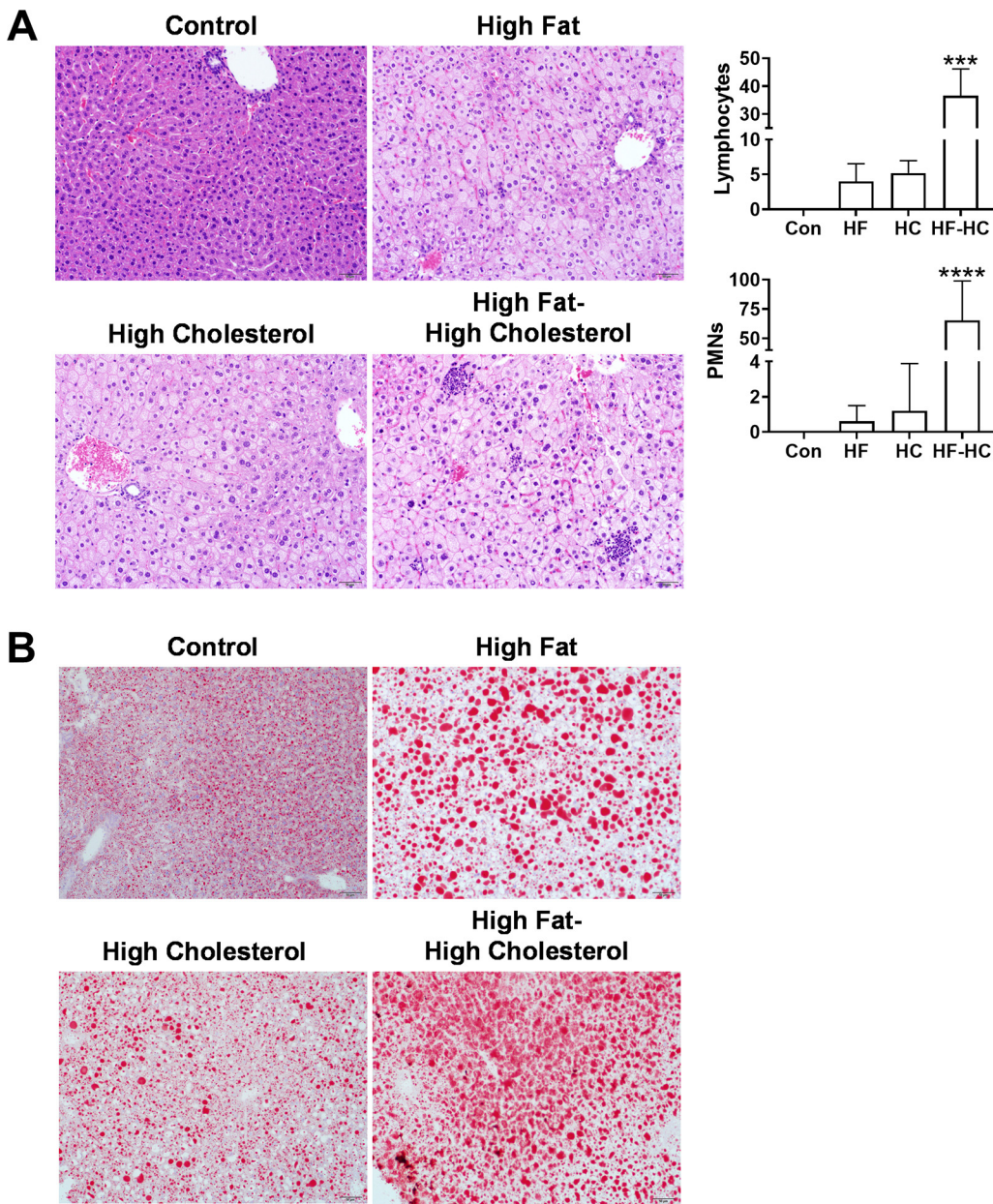


FIG 2 Diet impacts liver cellular composition and lipid content. (A) Organs were collected from uninfected BALB/c mice after 4 weeks of the experimental diets. Slides were prepared, and cells were counted by light microscopy. The images are representative of multiple slides. The numbers of total lymphocytes and polymorphonuclear leukocytes (PMNs) were counted in 10 high-power (magnification, $\times 1,000$) fields per uninfected mouse, and the sum for each mouse was calculated before calculating a mean for each group ($n=5$) (means and standard deviations) (***, $P < 0.0005$; ****, $P < 0.0001$ [by one-way ANOVA with a Dunnett posttest comparing uninfected mice fed experimental diets to uninfected mice fed the control {Con} diet]). HC, high cholesterol; HF, high fat; HF-HC, high fat-high cholesterol. (B) Tissues were collected from uninfected mice after 4 weeks of the experimental diets, and Oil-Red-O staining was performed. Images are representative of multiple slides.

Both macroscopic appearance and histological examinations indicated that the host microenvironment into which parasites were introduced was very different in mice fed the control versus experimental diets. This impression was verified by an overall assessment of transcriptomes of uninfected mice fed experimental diets. The mean F ratio when comparing the high-fat, high-cholesterol, or high-fat-high-cholesterol diet to the control diet was 3.34, 4.44, or 6.65, respectively. The mean F ratios of >1 led us to conclude that the experimental diets significantly contributed to the variance of the samples.

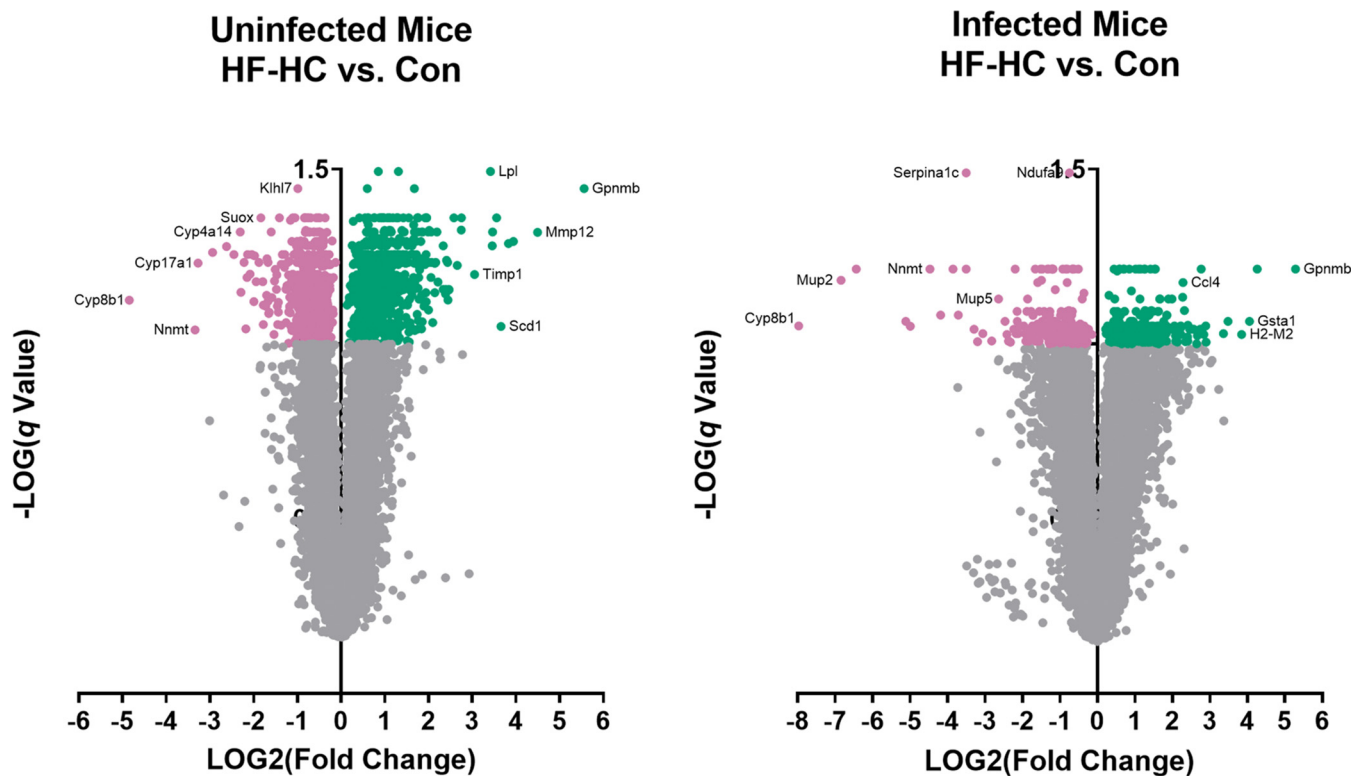


FIG 3 Transcript abundance in uninfected mice fed experimental diets. RNA extracted from the livers of uninfected and Li-infected mice fed various diets was examined using an Illumina MouseRef-8 V2.0 microarray. The resulting data were analyzed using Illumina Genome Studio and Partek. In Partek, one-way ANOVA was used to determine the differential abundances of transcripts. The transcript abundances in uninfected and Li-infected mice fed the experimental diets (high fat [HF], high cholesterol [HC], and high fat-high cholesterol [HF-HC]) were compared to those in uninfected and Li-infected mice fed the control (Con) diet, respectively. The fold change of each transcript was calculated in Partek ($n = 3$ for each diet). The P and q values were also calculated as a function of one-way ANOVA performed in Partek. All transcripts in the reference genome are depicted via a volcano plot, with significantly increased transcripts in green, significantly decreased transcripts in pink, and transcripts that did not significantly change in gray. A q value of <0.10 was considered significant ($n = 3$ mice for each diet).

Compared to uninfected mice fed the control diet, uninfected mice fed the high-fat, high-cholesterol, or high-fat-high-cholesterol diet had 1,812, 2,476, or 3,192 significantly changed (unadjusted P value of <0.05) transcripts, respectively. Using a false discovery rate (FDR) adjustment, there were 0, 2, or 1,274 significantly (q value of <0.10) changed transcripts in the livers of mice fed the high-fat, high-cholesterol, or high-fat-high-cholesterol diet, respectively (Fig. 3). Consistent with the magnitude and severity of differences in parasite load and histology, the greatest numbers of transcript changes were observed in the livers of mice fed the high-fat-high-cholesterol diet. The two transcripts that were significantly changed in uninfected mice fed the high-cholesterol diet were *2410002O22Rik* ($q = 0.0234413$, $P = 2.36E-06$, and fold change = 0.402691) and *Slc45a3* ($q = 0.0234413$, $P = 3.44E-06$, and fold change = 0.45553).

Comparisons of transcriptomes of Li-infected livers also revealed F ratios of >1 . The F ratio between infected mice fed the control diet and infected mice fed the high-fat, high-cholesterol, or high-fat-high-cholesterol diet was 3.34, 2.98, or 5.79, respectively. This further supports that the experimental diets significantly contributed to the variance in transcript abundance. Compared to infected animals fed a control diet, 1,806, 1,490, and 3,125 transcripts were significantly changed (unadjusted P value of <0.05) in infected animals fed high-fat, high-cholesterol, and high-fat-high-cholesterol diets, respectively. Again, using the FDR adjustment, 639 transcripts were significantly changed (q value of <0.10) in infected mice fed the high-fat-high-cholesterol diet compared to infected mice fed the control diet (Fig. 3). Mice fed either the high-fat or high-cholesterol diet had zero significantly changed transcripts (q value of <0.10).

TABLE 2 Pathway overrepresentation analysis of uninfected mice fed experimental diets^a

Diet	PANTHER pathway (PANTHER ID no.)	No. of transcripts		P value	FDR
		Observed	Expected		
High fat (decreased)	p53 pathway (P00059)	12	2.96	9.87E-05	8.19E-03
	Parkinson disease (P00049)	11	3.23	7.37E-04	3.06E-02
	FGF signaling pathway (P00021)	13	4.08	4.52E-04	2.50E-02
	Unclassified (unclassified)	627	668.74	1.26E-05	2.09E-03
High fat (increased)	No significant results				
High cholesterol (decreased)	Unclassified (unclassified)	859	914.32	8.17E-07	1.36E-04
High cholesterol (increased)	Circadian clock system (P00015)	5	0.44	3.11E-04	2.58E-02
	Inflammation mediated by chemokine and cytokine signaling pathway (P00031)	28	12.65	3.13E-04	1.73E-02
	Unclassified (unclassified)	912	964.68	4.03E-06	6.68E-04
High fat-high cholesterol (decreased)	Ubiquitin proteasome pathway (P00060)	14	3.71	7.55E-05	1.25E-02
	Unclassified (unclassified)	1,061	1,105.14	2.66E-04	2.21E-02
High fat-high cholesterol (increased)	Toll receptor signaling pathway (P00054)	20	3.89	5.29E-08	2.19E-06
	T cell activation (P00053)	28	6.36	2.21E-09	1.83E-07
	B cell activation (P00010)	20	4.95	1.29E-06	3.58E-05
	Apoptosis signaling pathway (P00006)	28	8.34	2.90E-07	9.63E-06
	VEGF signaling pathway (P00056)	15	4.88	3.63E-04	4.63E-03
	Ras pathway (P04393)	15	4.95	4.14E-04	4.91E-03
	Interleukin signaling pathway (P00036)	18	6.22	1.90E-04	2.63E-03
	Inflammation mediated by chemokine and cytokine signaling pathway (P00031)	50	18.24	3.85E-09	2.13E-07
	Cytoskeletal regulation by Rho GTPase (P00016)	15	5.58	1.23E-03	1.36E-02
	Angiogenesis (P00005)	31	11.95	9.06E-06	2.15E-04
	PDGF signaling pathway (P00047)	26	10.11	5.66E-05	9.40E-04
	EGF receptor signaling pathway (P00018)	24	9.61	1.53E-04	2.32E-03
	CCKR signaling map (P06959)	28	11.24	4.34E-05	8.00E-04
	Integrin signaling pathway (P00034)	33	13.43	1.51E-05	3.12E-04
p53 pathway (P00059)	15	6.15	3.74E-03	3.88E-02	
Unclassified (unclassified)	1,264	1,390.48	1.34E-18	2.22E-16	

^aObserved, number of transcripts in the data that represent a given pathway; expected, number of transcripts that are expected to represent a given pathway for a data list the size of the list entered; FGF, fibroblast growth factor; VEGF, vascular endothelial growth factor; CCKR, cholecystokinin receptor.

Pathway analyses further revealed inflammatory changes in the liver. To gain further insight into the mechanisms by which diet might influence the liver parasite burden, pathway analyses were performed using the PANTHER classification system. As pathway analyses are a more robust predictor of functional significance than individual transcripts considered as though they were independent markers, the above-described unadjusted *P* values were used for further analyses of pathways. Statistical overrepresentation and functional classification tests were performed using the PANTHER Pathways annotation set. The pathway analyses were performed on the 1,812, 2,476, and 3,192 transcripts significantly changed (*P* value of <0.05) in uninfected animals fed the high-fat, high-cholesterol, or high-fat-high-cholesterol diets as well as on 1,806, 1,490, and 3,125 transcripts significantly changed (*P* value of <0.05) in infected animals fed the high-fat, high-cholesterol, or high-fat-high-cholesterol diet.

Compared to mice fed the control diet, transcripts significantly increased in the livers of both uninfected and Li-infected mice fed the high-fat-high-cholesterol diet were significantly overrepresented in a number of pathways (Tables 2 and 3). Of particular interest are the overrepresented pathways related to immune function, which include T cell activation, B cell activation, the interleukin signaling pathway, and the Toll

TABLE 3 Pathway overrepresentation analysis of infected mice fed experimental diets^a

Diet	PANTHER pathway (PANTHER ID no.)	No. of transcripts		P value	FDR
		Observed	Expected		
High fat (decreased)	No significant results				
High fat (increased)	VEGF signaling pathway (P00056)	12	2.9	9.43E-05	7.83E-03
	Toll receptor signaling pathway (P00054)	9	2.31	1.02E-03	4.25E-02
	T cell activation (P00053)	12	3.78	8.33E-04	4.61E-02
	Unclassified (unclassified)	758	826.87	1.91E-10	3.16E-08
High cholesterol (decreased)	Blood coagulation (P00011)	8	5.97	1.24E-04	2.05E-02
High cholesterol (increased)	No significant results				
High fat-high cholesterol (decreased)	Pyrimidine metabolism (P02771)	6	0.62	1.72E-04	1.43E-02
	Blood coagulation (P00011)	18	2.88	1.45E-08	2.41E-06
	Unclassified (unclassified) ^b	1,066	1,111.32	1.94E-04	1.07E-02
High fat-high cholesterol (increased)	Toll receptor signaling pathway (P00054) ^b	20	3.77	3.24E-08	8.97E-07
	T cell activation (P00053) ^b	28	6.16	1.14E-09	6.33E-08
	VEGF signaling pathway (P00056) ^b	21	4.73	1.81E-07	3.77E-06
	Ras pathway (P04393) ^b	21	4.79	2.22E-07	4.09E-06
	B cell activation (P00010) ^b	20	4.79	8.16E-07	1.13E-05
	Cytoskeletal regulation by Rho GTPase (P00016) ^b	21	5.41	1.18E-06	1.50E-05
	Axon guidance mediated by semaphorins (P00007)	6	1.58	9.11E-03	5.04E-02
	Apoptosis signaling pathway (P00006) ^b	30	8.08	1.55E-08	5.15E-07
	Inflammation mediated by chemokine and cytokine signaling pathway (P00031) ^b	63	17.67	1.13E-15	9.37E-14
	Axon guidance mediated by netrin (P00009)	8	2.4	5.42E-03	3.46E-02
	EGF receptor signaling pathway (P00018) ^b	31	9.32	7.66E-08	1.82E-06
	CCKR signaling map (P06959) ^b	36	10.89	8.18E-09	3.39E-07
	Interferon gamma signaling pathway (P00035)	7	2.12	9.59E-03	4.98E-02
	FGF signaling pathway (P00021)	27	8.22	6.46E-07	1.07E-05
	Histamine H1 receptor-mediated signaling pathway (P04385)	10	3.08	2.35E-03	1.70E-02
	Interleukin signaling pathway (P00036) ^b	19	6.03	4.61E-05	4.50E-04
	Angiotensin II-stimulated signaling through G proteins and beta-arrestin (P05911)	8	2.67	9.38E-03	5.02E-02
	5HT1-type receptor-mediated signaling pathway (P04373)	9	3.01	6.11E-03	3.63E-02
	Oxytocin receptor-mediated signaling pathway (P04391)	12	4.04	1.74E-03	1.37E-02
	Parkinson disease (P00049)	19	6.51	1.12E-04	1.03E-03
	p53 pathway (P00059) ^b	17	5.96	3.20E-04	2.79E-03
	Thyrotropin-releasing hormone receptor signaling pathway (P04394)	12	4.25	2.49E-03	1.66E-02
	PI3 kinase pathway (P00048)	10	3.56	5.76E-03	3.54E-02
	5HT2-type receptor-mediated signaling pathway (P04374)	13	4.66	1.85E-03	1.40E-02
	Angiogenesis (P00005) ^b	32	11.58	1.72E-06	1.90E-05
	PDGF signaling pathway (P00047) ^b	27	9.79	1.13E-05	1.17E-04
	Integrin signaling pathway (P00034) ^b	35	13.01	1.31E-06	1.56E-05
Endothelin signaling pathway (P00019)	15	5.62	1.27E-03	1.05E-02	
Gonadotropin-releasing hormone receptor pathway (P06664)	41	16.16	6.73E-07	1.02E-05	
Huntington disease (P00029)	22	10.27	2.42E-03	1.68E-02	
Heterotrimeric G-protein-signaling pathway-Gq alpha- and Go alpha-mediated pathway (P00027)	17	8.29	8.32E-03	4.76E-02	
Unclassified (unclassified) ^b	1,187	1,347.19	1.24E-28	2.06E-26	

^aObserved, number of transcripts in the data that represent a given pathway; expected, number of transcripts that are expected to represent a given pathway for a data list of the size of the list entered; PI3, phosphatidylinositol 3.

^bPathway also overrepresented in uninfected mice fed the same diet.

receptor signaling pathway (Tables 2 and 3). While many of these pathways did not reach significant overrepresentation in mice fed the high-fat or high-cholesterol diet, the functional classification tests denoted changes in these pathways for these diets (Fig. 4). Changes in the angiogenesis pathway are also of interest (Tables 2 and 3 and Fig. 4), given that angiogenesis has been associated with organomegaly (25) and given that the WHO cites hepatomegaly as a signature symptom of VL (26).

While eight of the most significantly overrepresented pathways in the livers of Li-infected mice fed the high-fat–high-cholesterol diet were also significantly overrepresented in uninfected mice fed the same diet, a number of pathways were not shared between infected and uninfected mice fed the high-fat–high-cholesterol diet (Tables 2 to 5). For instance, in Li-infected mice fed the high-fat–high-cholesterol diet, the interferon gamma (IFN- γ) signaling pathway was significantly overrepresented ($P=0.00959$; FDR=0.0498) compared to Li-infected mice fed the control diet (Table 3). But this pathway was not overrepresented in uninfected mice fed the same diet. Because the patterns observed in uninfected mice fed the experimental diets were exacerbated in infected mice fed the experimental diets, we can conclude that diet and infection likely synergistically played a role in the phenotypic changes.

Examination of transcripts of interest via qPCR. Several transcripts of interest were examined by qPCR. Uninfected mice fed the control diet served as the mathematical control during the comparative threshold cycle (C_T) method (Fig. 5). Further statistical comparisons were made between infected mice fed the control diet and infected mice fed the experimental diets. We acknowledge that, individually, several of our transcripts of interest may not have significantly changed in the mice. However, in concert with other transcript changes, our transcripts of interest may have impacted functional pathways and the outcome of infection.

The expression of *stat1* in infected mice fed either the high-fat or the high-fat–high-cholesterol diet was significantly increased compared to that in infected mice fed the control diet. The expression of *Nfkb1a* was significantly increased in infected mice fed the high-fat–high-cholesterol and showed only a trend toward decreased expression in mice fed the high-cholesterol diet. Consistently, the expression of *nfkb1* trended toward increased expression in mice fed the high-cholesterol diet, and there was a lack of change in mice fed the high-fat–high-cholesterol diet. The only other transcript reaching statistical significance among our chosen gene products was *il1b*. Amplification of this transcript could reflect either the differing cellular compositions of livers induced by the high-fat–high-cholesterol diet, upregulation in endogenous cells of the liver (Kupffer and stellate cells), or both.

Other transcripts of interest did not reach statistical significance, but this does not rule out the possibility that these contributed to the significant upregulation of a functional pathway. These transcripts that did not reach significance, only some of which are shown, included *nfkb1*, *fcgr4*, *ifi30*, *myd88*, *il1a*, and *ccl7*. *Fgr3* and *ccl3* transcripts did not show a trend toward significance, and the error bars for *tlr2* transcript data were so high as to be nonconvincing. A full microarray was not repeated, but a microarray on three independent mice per experimental diet revealed the differential expression of *Fcgr4*, *Stat1*, *IFI30*, *IL1b*, and *Tlr2* at a statistically significant level, with fold changes 2.98-, 1.01-, 2.54-, 2.53-, and 7.47-fold higher than those of mice fed a control diet.

DISCUSSION

The changing prevalences of obesity and food insecurity in areas where leishmaniasis is endemic (18, 19) likely reflect changing dietary habits and access to health care. However, the impacts of diet composition on visceral leishmaniasis are not fully understood. Previous evidence of the impacts of dietary lipids on parasitic disease includes a study of C57BL/6 mice fed a high-lipid diet prior to *Plasmodium berghei* infection, which led to increased survival and reduced parasitemia (27). Studies of *Trypanosoma cruzi* have led to mixed results: CD-1 mice fed a high-fat diet prior to or coincident with *T. cruzi* infection had increased survival rates (28, 29). In contrast, CD-1 mice fed that same high-fat diet experienced worsened cardiac disease when infected with a lower dose of the same *T. cruzi* strain (30), and mice

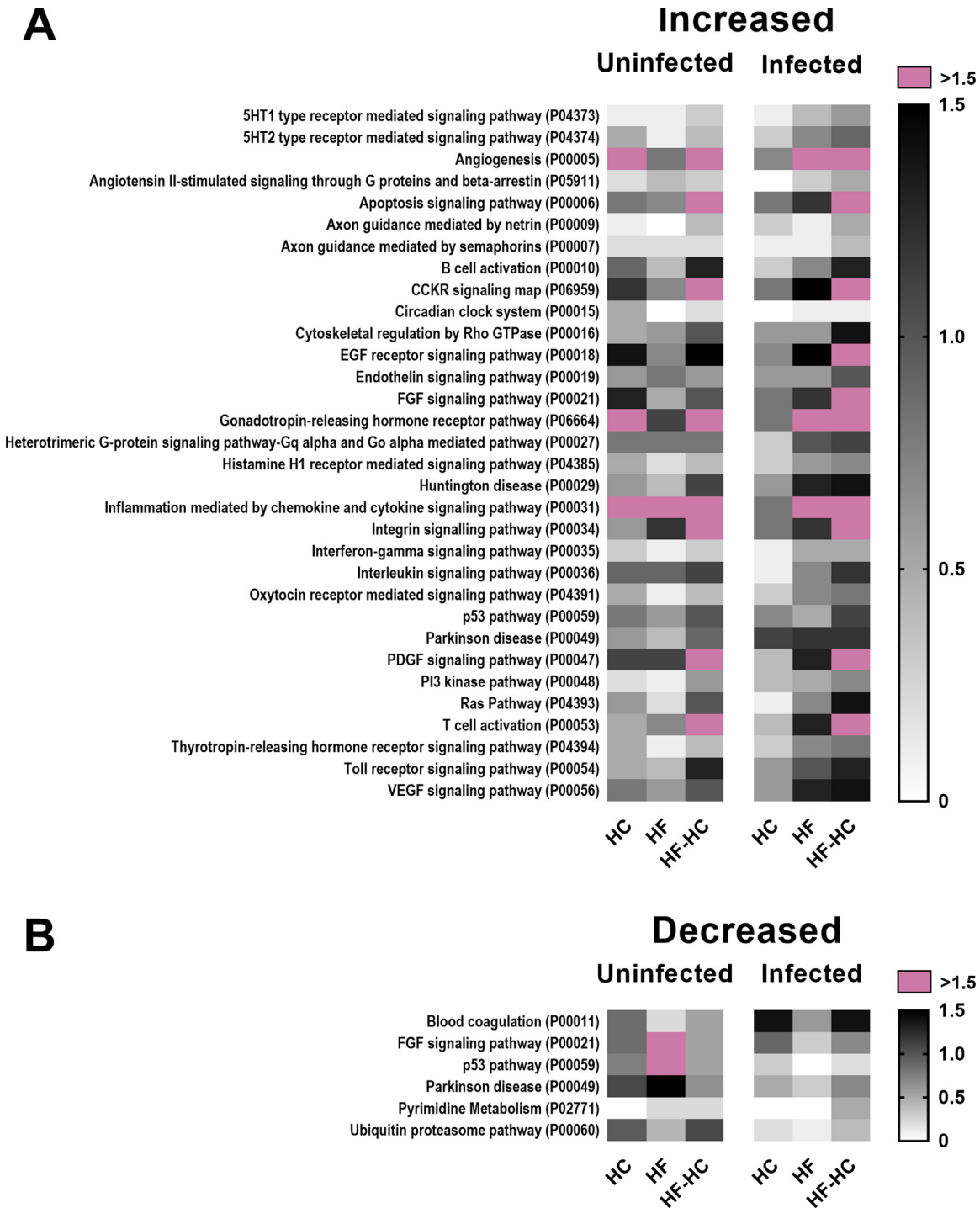


FIG 4 Pathway analyses of increased transcripts. Transcripts found to be significantly ($P < 0.05$) increased (A) or decreased (B) via one-way ANOVA when mice fed the experimental diets were compared to mice fed a control diet were analyzed using functional classification tests via the PANTHER classification system. The PANTHER pathway identification number (in parentheses) is included with the name of the pathway. For each diet, the percentage of significantly changed transcripts that represent a given pathway was graphed (the key depicts 0% to 1.5%). Pathways for which more than 1.5% of transcripts were representative are in pink. Fewer than 4.5% of transcripts were assigned to any given pathway. Only pathways that the statistical overrepresentation tests found to be significantly overrepresented in at least one of the experimental diets fed to either infected or uninfected mice are included ($n = 3$ uninfected and infected mice for each experimental diet). HC, high cholesterol; HF, high fat; HF-HC, high fat-high cholesterol.

TABLE 4 The most significant pathways and their transcripts with differential abundances in uninfected mice^a

Diet	PANTHER pathway (PANTHER ID no.)	FDR	Transcripts
High fat (decreased)	p53 pathway (P00059)	8.19E-03	<i>Pten Traf6 Ppp2ca Bai3 Cdkn1a Thbs1 Mr1 Sumo3 Pik3r3 Kat2b Ccne1 Pik3c2g</i>
	FGF signaling pathway (P00021)	2.50E-02	<i>Map2k4 Ppp6c Mapk1 Ppp2r1a Map2k6 Ywhaz Ppp2ca Ptpn11 Ppp2r5c Ppp2r5e Ywhaq Pik3c2g Shc1</i>
	Parkinson disease (P00049)	3.06E-02	<i>Hspa9 Mapk1 Ywhaz Src Sept2 Csnk2a1 Pasma4 Hspa11 Ywhaq Ccne1 Hspa8</i>
High cholesterol (increased)	Inflammation mediated by chemokine and cytokine signaling pathway (P00031)	1.73E-02	<i>Ccl21a Nfat5 Ifngr2 Ltb4r2 Junb Prkcb Alox12 Mapk3 Il1b Rgs1 Ccr10 Vav1 Myh9 Il15 Prkcz Il10rb Itga9 Plcg2 Mylk Camk2g Inpp1 Il8ra Dclk3 Itpr2 Grb2 Ccl27 Itga4 Alox15</i>
	Circadian clock system (P00015)	2.58E-02	<i>Per1 Cry2 Csnk1e Csnk1d Per2</i>
High fat-high cholesterol (decreased)	Ubiquitin proteasome pathway (P00060)	1.25E-02	<i>Psmc1 Ube2e2 Ube2g1 Psmd12 Hip2 Ube2d2 Psmd9 Psmd14 Ube2e3 Uchl5 Ube2d3 Ube2a Psmd1 Ube1x/Uba1</i>
High fat-high cholesterol (increased)	T cell activation (P00053)	1.83E-07	<i>Pik3cb Ppp3cc Calm3 Ptprc Map3k1 Pik3r2 Mapk3 Lat Cd3g Vav1 Fos H2-DMb1 Pik3cd B2m Cd3e Cd74 Mapk9 Nras Nfatc4 Nfkbia Lcp2 Cd86 Csk H2-Ea Nfkb1 Akt3 H2-DMa Rac2</i>
	Inflammation mediated by chemokine and cytokine signaling pathway (P00031)	2.13E-07	<i>Prkx Pak4 Ccl7 Nfat5 Ifngr2 Pik3cb Itgb7 Junb Prkcb Il1f6 Arpc1b Mapk3 Il1b Alox5ap Rgs1 Vav1 Pik3cd Myh9 Gnai2 Il15 Jak2 Il10rb Col6a1 Ikbke Cxcl10 Itga9 Adrbk1 Plcg2 Camk2g Myh8 Tyk2 Inpp1 Nras Nfatc4 Nfkbia Plcb3 Cxcr4 Ccl5 Ccl27 Fpr2 Ccl2 Plcl2 Nfkb1 Akt3 Cx3cr1 Fpr2 Ccl4 Shc1 Rela Rac2</i>
	Toll receptor signaling pathway (P00054)	2.19E-06	<i>Map3k8 Tlr8 Myd88 Map3k1 Mal Tnfaip3 Mapk3 Tlr2 Mapk9 Ikbke Tlr7 Irf3 Tcam1 Cd14 Nfkbia Irak3 Irf7 Nfkb1 Tbk1 Rela</i>
	Apoptosis signaling pathway (P00006)	9.63E-06	<i>Ripk1 Mcl1 Bcl2a1c Bcl2l11 Pik3cb Map3k1 Prkcb Apaf1 Mapk3 Fos Pik3cd Prkcd Eif2ak2 Traf2 Bag1 Mapk9 Bcl2a1d Atf3 Mcm5 Bok Map3k14 Nfkbia Bcl2l2 Nfkb1 Birc2 Akt3 Rela Tmbim6</i>
	B cell activation (P00010)	3.58E-05	<i>Cd22 Pik3cb Ppp3cc Calm3 Ptprc Prkcb Btk Map3k3 Mapk3 Vav1 Fos Pik3cd Prkcd Mapk9 Plcg2 Nras Nfatc4 Nfkbia Nfkb1 Rac2</i>
	Angiogenesis (P00005)	2.15E-04	<i>Grb7 Mapkapk3/Mapk3 Rhob Pik3cb Pdgfrb Prkd2 Map3k1 Prkcb Arhgap1 Rasa1 Pik3r2 Dok3 Mapk3 Ctnnb1 Fos Pik3cd Dok2 Notch4 Lpxn Pdgfa Prkcd Pdgfb Pld1 Plcg2 Vegfa Nras Angpt2 Akt3 Sh2d2a Dvl1 Shc1</i>
	Integrin signaling pathway (P00034)	3.12E-04	<i>Rap2b Rhob Pik3cb Itgb7 Map3k1 Col4a1 Arpc1b Itgae Col3a1 Pik3r2 Map3k3 Itgb4 Mapk3 Col1a1 Pik3cd Itgax Itgb5 Col5a1 Lamc1 Col16a1 Mapk9 Col6a1 Itga9 Flna Col15a1 Elmo1 Scara3 Nras Csk Col4a2 Shc1 Rac2 Actn1</i>
	CCKR signaling map (P06959)	8.00E-04	<i>Plau Mcl1 Tpcn2 Pik3cb Prkd2 Arhgap4 Prkcb Hdc Map3k11 Mapk3 Ctnnb1 Fos Csnk1e Prkcd Jak2 Mapk9 Cdh1 Tcf4 Map3k14 Csnk1d Nfkbia ler3 Ccnd1 Csk Birc2 Rps6ka1 Shc1 Hdac7</i>
	PDGF signaling pathway (P00047)	9.40E-04	<i>Stat4 Rhob Pik3cb Pdgfrb Jak3 Arhgap4 Nin Arhgap1 Rasa1 Pik3r2 Mapk3 Rps6kl1 Vav1 Fos Pik3cd Pdgfa Pdgfb Erf Jak2 Mknk2 Plcg2 Arhgap9 Elf5 Nras Rps6ka1 Shc1</i>
	EGF receptor signaling pathway (P00018)	2.32E-03	<i>Gab3 Cdk2 Btc Stat4 Areg Pik3cb Rhoj Prkd2 Map3k1 Prkcb Rasa1 Map3k3 Mapk3 Pik3cd Prkcd Mapk9 Plcg2 Nras Dab2ip Ywhah Akt3 Nrg1 Shc1 Rac2</i>

^aFor increased and decreased transcripts in each diet, only the 10 most significantly overrepresented pathways are included.

TABLE 5 The most significant pathways and their transcripts with differential abundances in infected mice^a

Diet	PANTHER pathway (PANTHER ID no.)	FDR	Transcripts
High fat (increased)	VEGF signaling pathway (P00056)	7.83E−03	<i>Mapkapk2 Pla2g4a Mapkapk3 Mapk1 Arhgap1 Lpxn Ets1 Prkch Nras Sh2d2a Rac2 Prr5</i>
	Toll receptor signaling pathway (P00054)	4.25E−02	<i>Mapk1 Tlr4 Tnfaip3 Tollip Tank Tlr7 Cd14 Nfkb1 Rela</i>
	T cell activation (P00053)	4.61E−02	<i>H2-Oa Mapk1 Fos H2-DMb1 Cd3d Cd74 Nfatc1 Nras Cd86 H2-Ea Nfkb1 Rac2</i>
High cholesterol (decreased)	Blood coagulation (P00011)	2.05E−02	<i>F11 F13b F8 Serpina1d Plaur Plg F5 Serpina1c</i>
High fat-high cholesterol (decreased)	Blood coagulation (P00011)	2.41E−06	<i>Fga F11 Serpina1e Serpina1b Klkb1 F9 F12 F8 Serpina1a F7 Serpina1d Plg Kng2 F5 Serpina1c Serpinf2 Proz Serpind1</i>
	Pyrimidine metabolism (P02771)	1.43E−02	<i>Upb1 Nt5e Abat Dpys Aldh6a1 Dpyd</i>
High fat-high cholesterol (increased)	Inflammation mediated by chemokine and cytokine signaling pathway (P00031) ^b	9.37E−14	<i>Plcb2 Prkx Pik3cg Pak4 Stat3 Ccl7 Actb Cish Ifngr2 Pik3cb Itgb7 Bcl3 Junb Cdc42 Prkcb Arpc1b Il8rb Alox12 Arpc5 Mapk3 Il1b Alox5ap Rgs1 Ccr6 Vav1 Plch1 Pik3cd Myh9 Ccl3 Cxcl4 Ccr5 Ikbke Nfkbie Relb Adrbk1 Plcg2 Mylk Rac1 Arrb2 Vwf Nfatc1 Ptk2b Tyk2 Itgb2 Prkacb Inpp11 Nras Nfkbia Plcb3 Cxcr4 Ccl5 Fpr2 Ccl2 Cx3cr1 Fpr2 Alox15 Ccl4 Akt1 Stk4 Shc1 Rela Rac2 Gng2</i>
	T cell activation (P00053) ^b	6.33E−08	<i>Pik3cg H2-Oa H2-Aa Lck Pik3cb Calm3 Cdc42 Map3k1 Mapk3 Lat Vav1 Fos H2-DMb1 Pik3cd Cd3d B2m Cd3e Cd74 Rac1 Nfatc1 Nras Nfkbia Cd86 H2-Ea Akt1 Stk4 Pik3r1 Rac2</i>
	CCKR signaling map (P06959) ^b	3.39E−07	<i>Plau Stat3 Mcl1 Pik3cb Prkd2 Arhgap4 Cdc42 Prkcb Srf Hdc Mapk3 Ctnnb1 Fos Csnk1e Prkcd Ptpn11 Ywhab Prkch Cdh1 Rac1 Arrb2 Rgs2 Ptk2b Mmp9 Prkacb Tcf4 Csnk1d Nfkbia Ier3 Ccnd1 Rps6ka1 Egr1 Akt1 Pik3r1 Shc1 Gng2</i>
	Apoptosis signaling pathway (P00006) ^b	5.15E−07	<i>Pik3cg Crebl1 Mcl1 Bcl2a1c Bcl2l11 Jdp2 Pik3cb Map3k1 Prkcb Apaf1 Tnf Mapk3 Daxx Fos Pik3cd Map4k4 Prkcd Prkch Eif2ak2 Bag1 Relb Bcl2a1d Atf3 Bok Gck Nfkbia Fadd Akt1 Rela Tnfrsf10b</i>
	Toll receptor signaling pathway (P00054) ^b	8.97E−07	<i>Tlr4 Myd88 Map3k1 Tirap Tnfaip3 Ly96 Mapk3 Tlr2 Ikbke Nfkbie Tlr7 Irak4 Cd14 Tlr1 Nfkbia Irak3 Irf7 Tbk1 Rela Ticam2</i>
	EGF receptor signaling pathway (P00018) ^b	1.82E−06	<i>Gab3 Pik3cg Stat3 Stat4 Areg Pik3cb Prkd2 Cdc42 Map3k1 Prkcb Ywhaz Rasa1 Mapk3 Ppp2ca Pik3cd Prkcd Osm Ywhab Prkch Plcg2 Rac1 Pik3r6 Ppp4c Nras Dab2ip Ppp2r5c Ywhah Nrg1 Akt1 Shc1 Rac2</i>
	VEGF signaling pathway (P00056) ^b	3.77E−06	<i>Pik3cg Mapkapk3/Mapk3 Pik3cb Prkd2 Prkcb Arhgap1 Mapk3 Mapk6 Pik3cd Lpxn Prkcd Ets1 Prkch Plcg2 Rac1 Nras Sh2d2a Akt1 Pik3r1 Rac2 Prr5</i>
	Ras pathway (P04393) ^b	4.09E−06	<i>Pik3cg Mapkapk3/Mapk3 Stat3 Pik3cb Cdc42 Map3k1 Srf Mapk3 Pik3cd Ets1 Ralb Pld1 Rac1 Nras Rgl2 Rps6ka1 Exoc2 Akt1 Stk4 Shc1 Rac2</i>
	Gonadotropin-releasing hormone receptor pathway (P06664)	1.02E−05	<i>Vcl Stat3 Gata2 Map3k9 Tgif1 Dgkz Mmp14 Junb Cdc42 Map3k1 Prkcb Esrra Srf Adcyap1 Mapk3 Ctnnb1 Skil Ldb1 Fos Anxa5 Pgr Map4k4 Tuba6 Prkcd Map3k12 Smad3 Rac1 Nfatc1 Ptk2b Atf3 Gnb4 Gck Rap1b Alox15 Egr1 Akt1 Pik3r1 Rela Smad1 Cnp Gng2</i>
	FGF signaling pathway (P00021)	1.07E−05	<i>Pik3cg Pik3cb Cdc42 Map3k1 Prkcb Ywhaz Rasa1 Map3k6 Mapk3 Ppp2ca Pik3cd Prkcd Ptpn11 Ywhab Prkch Plcg2 Rac1 Ppp4c Ppp4r1 Nras Ptpn6 Ppp2r5c Fgf5 Ywhah Akt1 Shc1 Rac2</i>

^aFor increased and decreased transcripts in each diet, only the 10 most significantly overrepresented pathways are included.

^bPathway also overrepresented in uninfected mice fed the same diet.

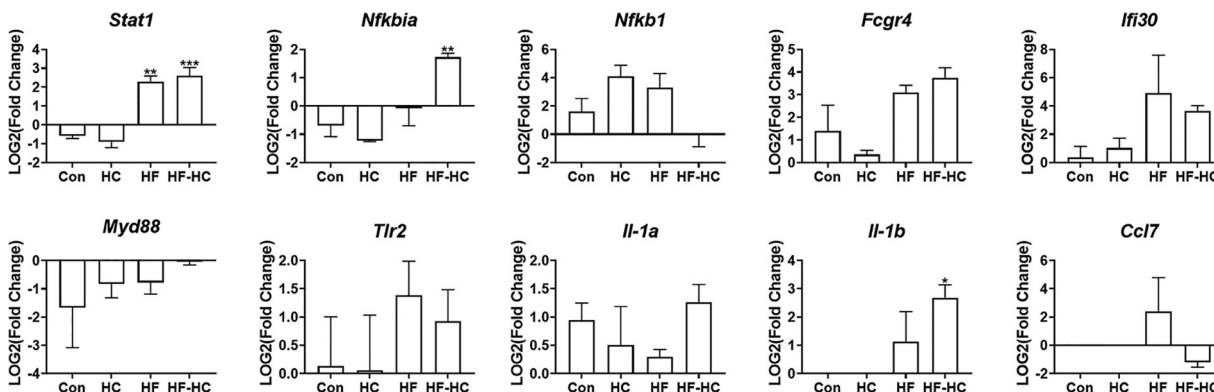


FIG 5 qPCR validation of transcript expression in infected mice. Using SYBR green qPCR, the abundance of transcripts was validated to further examine the changes in infection severity due to diet. For each mouse, the mean of 3 replicate C_T values for each transcript of interest was calculated. Using the comparative C_T method, the fold change of each transcript was determined by comparing infected mice fed one of the four diets (control [Con], high cholesterol [HC], high fat [HF], and high fat-high cholesterol [HF-HC]) to uninfected mice fed the control diet. *gapdh* was used as the internal control. ($n = 3$) (means and SEM) (*, $P < 0.05$; **, $P < 0.005$; ***, $P < 0.0005$ [by one-way ANOVA with a Dunnett posttest comparing infected mice fed the experimental diets to infected mice fed the control diet]).

fed a high-fat diet and infected with a different strain of *T. cruzi*, VL-10, had increased parasite loads (31).

Studies of *Leishmania* spp. have similarly shown conflicting results. Like with *T. cruzi* VL-10, C57BL/6 mice fed a high-sugar and -butter diet had increased *L. infantum* burdens in their livers and spleens after 8 weeks of infection (21), but *L. donovani*-infected C57BL/6 mice fed a high-fat-high-cholesterol diet had significantly reduced parasite burdens (20). Because the impact of dietary lipids specifically on the outcome of VL remains poorly characterized and contradictory, we examined the hypothesis that dietary lipid intake would impact the severity and outcome of chronic Li infection.

Similar to the above-mentioned studies, the present study showed that increased dietary lipid intake via any of three experimental diets reduced Li liver parasite burdens after 4 weeks of infection compared to infected mice fed a control diet. More specifically, liver parasite burdens were significantly decreased and nearly undetectable in mice fed the high-fat-high-cholesterol diet. Our data also showed significant increases in splenic parasite burdens after 8 weeks of infection in mice fed the high-fat-high-cholesterol diet. These data raised the possibility that tissue-specific responses and kinetics of infection matter in the outcome of VL. Together, these data suggested that there may be an immediate protective effect of diet on Li infection but that chronic infection could be promoted by the high-lipid diet. Histological examination showed an inflammatory response in mice fed the high-fat-high-cholesterol diet.

Also of note, other experiments by our group and other investigators show that granulomatous responses are associated with the clearance of parasites in murine leishmaniasis (22). We observed a predominance of polymorphonuclear rather than mononuclear leukocytes in the livers of mice fed the high-fat-high-cholesterol diet, and we suspect that this aberrant cellular response resulting from the high-fat-high-cholesterol diet would more likely be associated with parasites failing to establish infection in the liver rather than granuloma-associated clearance of parasites.

To characterize the effect of excess lipid intake specifically during experimental VL, we examined the transcriptomes of liver tissues of mice fed the three different experimental diets. Uninfected mice fed the high-fat-high-cholesterol diet had transcripts that specified the overexpression of genes related to chemokines and their receptors in inflammatory responses. Other pathways or groups of genes whose expression was significantly upregulated in both uninfected and infected mice fed the combined high-fat-high-cholesterol diet included Toll receptor signaling pathways, T cell activation, B cell activation, interleukin signaling pathways, and integrin signaling pathways. These results demonstrate that even prior to infection, the livers of mice fed the high-lipid diets had become an inflammatory environment.

Also of interest and in need of further investigation, angiogenesis, which often accompanies organomegaly (25), was significantly overrepresented in both uninfected and Li-infected mice fed the high-fat–high-cholesterol diet. Furthermore, our histological sections showed considerable steatoses in all diets, which were likely stellate cell lipid bodies. Consistent with the involvement of stellate cells as well as endothelial and epithelial cell proliferation, platelet-derived growth factor (PDGF) and epidermal growth factor (EGF) receptor signaling pathways were overrepresented by transcripts from the livers of uninfected and Li-infected mice fed the high-fat–high-cholesterol diet. Both pathways are associated with angiogenesis but are not, by any means, the only drivers (32).

We hypothesize that the hepatic inflammatory and proangiogenesis environment might underlie the apparent protected or refractory state of livers observed in Li-infected mice fed the experimental diets, especially in mice fed the high-fat–high-cholesterol diet. A few studies of mice coinfecting with microorganism-induced inflammatory stimuli have demonstrated similar phenomena. Infection with the helminthic pathogen *Trichinella spiralis* or *Trichuris muris* prior to infection with *Leishmania* spp. reduced *Leishmania* parasite burdens in murine livers, possibly due to increased inflammatory mediators such as interleukin 4 (IL-4) and IFN- γ (33, 34). In contrast, prior infection with another helminth, *Schistosoma mansoni*, led to increased *L. donovani* burdens in both livers and spleens (35).

As opposed to the above-described coinfections in murine models of VL, infection with *Staphylococcus aureus* in the skin prior to infection with *L. major*, a cause of cutaneous leishmaniasis (4), had no significant effect on the parasite burden in the ear but significantly exacerbated the severity of inflammatory skin lesions 4 weeks after coinfection (36). Therefore, we tentatively conclude that the nature of the inflammatory stimulus coinciding with *Leishmania* infection and the resultant activated immune mediators will likely lead to distinct effects on the course of leishmaniasis, depending on whether the immune responses induced by the costimulus suppresses or synergizes with pathological responses to the *Leishmania* species.

Utilizing the comparison with diet as the single independent variable, we were able to observe that eight of the most significantly overrepresented pathways in Li-infected mice fed the high-fat–high-cholesterol diet were also significantly overrepresented in uninfected mice fed the same diet. We can therefore conclude that the observed increase in these pathways may have been largely influenced by diet and not solely due to subsequent infection by Li. Very briefly, the sorting of *mapk3* into each of the 10 most significantly overrepresented pathways in the infected mice fed the high-fat–high-cholesterol diet is another interesting observation that we were able to make with this comparison.

To summarize, the interplay between excess dietary lipid intake and consequent aberrant inflammatory changes and chronic infections is not well defined. The data presented here show that increased dietary lipid intake leads to inflammatory changes and, thus, changes in the infection kinetics and severity of chronic VL. Prolonged and increased dietary fat and cholesterol in combination provided a localized protective effect against the expansion of parasites causing VL, leading to reduced parasite burdens in the livers. However, parasite loads significantly increased in spleens of mice fed the high-fat–high-cholesterol diet, the site where parasites are maintained long term in the infected host (37, 38).

What we cannot discern from the current study is whether the ultimate effects of elevated-lipid diets on chronic infection, in this case, in the spleens of infected mice, might be a prolongation of the chronic carrier state rather than amelioration of disease. The study raises the possibility that temporary changes in dietary lipid intake might enhance the proinflammatory environment acutely during treatment, possibly providing an additive approach to treatment along with antiparasitic agents. Our next challenges are to determine whether dietary changes similarly change parasite loads in human hosts and to discern other conditions under which similar changes caused by dietary intake cause important changes in disease outcomes.

MATERIALS AND METHODS

Experimental groups. Female BALB/c mice were maintained on the following diets: control (standard, 18% protein diet, with 4% fat and <0.04% cholesterol), high fat (diet TD.88137; 21.2% fat and 0.2%

cholesterol), high cholesterol (TD.01383; 5.7% fat and 2% cholesterol), or high fat-high cholesterol (TD.02028; 21.2% fat and 1.3% cholesterol). Mice were started on their respective diets 4 weeks prior to infection. The diets were obtained from Envigo (Indianapolis, IN). The macronutrients of each diet are listed in Table 1.

Histology. Liver tissue was collected after 4 weeks on each diet. The tissues were then sectioned and fixed. Fixed samples were stained with hematoxylin and eosin (H&E) as well as Oil-Red-O. Slides were then examined by light microscopy, and 10 high-power fields were chosen at random in uniform quadrants on each slide. Leukocyte composition was enumerated in all 10 fields and summed for each mouse. The average number of leukocytes was calculated for each diet.

Infection and monitoring of infection dynamics. A strain of Li isolated from a patient with visceral leishmaniasis in Brazil (MHOM/BR/00/1669) was maintained by serial passage in hamsters. Metacyclic promastigotes were isolated by Percoll density gradients as we previously described (39). Mice were infected with 1×10^6 metacyclic, recombinant Li promastigotes expressing firefly luciferase via intravenous injection in the tail 4 weeks after the onset of the experimental diets. An *in vivo* imaging system (IVIS) was used to monitor the trafficking and expansion of parasite loads. Images were collected with the Xenogen IVIS 200 system. At weekly time points, animals were anesthetized with isoflurane and inoculated with luciferin by intraperitoneal injection 10 min prior to imaging. Parasite localization was assessed using Living Image software (40). The representative images included here were taken at 4 weeks postinfection.

qPCR quantification of parasite burden. At 4 and 8 weeks postinfection, groups of five mice from each diet were euthanized, livers and spleens were homogenized, and DNA was extracted as we previously described (41). Parasite loads in each organ were determined via quantitative PCR (qPCR) using the kDNA7 primers and probe described previously by Weirather et al. (41).

Transcriptomes. After 12 weeks of each diet (8 weeks after infection or PBS injection), mice were euthanized, and RNA was extracted from liver tissues. Each experimental group, uninfected and infected mice fed any of the four diets, included three biological samples, totaling 24 mice. Total RNA was purified using the TRIzol method followed by DNase treatment and Qiagen column purification, and transcriptional profiles were measured via Illumina MouseRef-8 V2.0 microarrays at the Iowa Institute of Human Genetics, Genomics Sequencing Division, University of Iowa.

After quality control, a custom report was made of the raw microarray data using Illumina GenomeStudio V2011.1 (42). The report was then imported into Partek 7.19.1125 (43) using the gene expression workflow. Samples were annotated with attributes, and separate spreadsheets were created for each comparison to be made. Because we were examining more samples than could fit on one Illumina bead chip, principal-component analyses and histograms were assessed to ensure that samples clustered by experimental group rather than by chip. No samples were removed in this assessment.

By individually comparing each experimental diet to the control diet, differentially expressed transcripts were determined using one-way analysis of variance (ANOVA), and the source of variation of transcript expression was examined. *q* values, FDR-adjusted *P* values, were then calculated and are depicted as volcano plots. Gene lists were exported and included all transcripts that could be found in the reference library so that further analyses could be completed. For further analyses, transcripts with a *P* value of 0.05 were considered significantly differentially expressed.

Validation of the differential expression of transcripts of interest was performed using SYBR green qPCR on the samples used for the murine microarray. The comparative C_T method was used to calculate a fold change for each transcript (44). More specifically, the fold change between infected mice fed the control diet or the experimental diets and uninfected mice fed the control diet was calculated. *gapdh* was used as the internal control.

Pathway analyses. Transcripts found to be significantly changed ($P < 0.05$) by each experimental diet were entered into the PANTHER classification system (45–47). Both statistical overrepresentation and functional classification tests were performed. For both tests, the PANTHER Pathways annotation set was used. For statistical overrepresentation tests, *Mus musculus* was selected as the default whole-genome list, and the Fisher test was used with an FDR correction. Data were exported as .txt files to be further analyzed.

Further statistical analyses. GraphPad Prism 8.4.3 (48) was utilized for further statistical analysis of data. When appropriate, one- and two-way ANOVAs were completed, and outliers were identified with ROUT.

Ethical approval. All studies using vertebrate animals for research were first reviewed and approved by institutional review boards at the Iowa City Department of Veterans' Affairs Medical Center (Animal Component of Research Protocol [ACORP] 2090301 and ACORP 1890601) and the University of Iowa (protocol ACURF 0081099).

ACKNOWLEDGMENTS

These studies were funded in part by grants BX001983 and BX000536 from the Department of Veterans' Affairs Research and Development (M.E.W.). The work was conducted while E.T.K. was funded by grant T32 AI007511 from the National Institutes of Health. The funders had no role in study design, data collection and analysis, decision to publish, or preparation of the manuscript.

We are grateful to Noah Butler and Lilliana Radoshevich for their helpful reviews of the manuscript.

REFERENCES

- World Health Organization. 2016. Leishmaniasis in high-burden countries: an epidemiological update based on data reported in 2014. *Wkly Epidemiol Rec* 22:287–296.
- Okwor I, Uzonna J. 2016. Social and economic burden of human leishmaniasis. *Am J Trop Med Hyg* 94:489–493. <https://doi.org/10.4269/ajtmh.15-0408>.
- Herwaldt BL. 1999. Leishmaniasis. *Lancet* 354:1191–1199. [https://doi.org/10.1016/S0140-6736\(98\)10178-2](https://doi.org/10.1016/S0140-6736(98)10178-2).
- Kaye P, Scott P. 2011. Leishmaniasis: complexity at the host-pathogen interface. *Nat Rev Microbiol* 9:604–615. <https://doi.org/10.1038/nrmicro2608>.
- Koff AB, Rosen T. 1994. Treatment of cutaneous leishmaniasis. *J Am Acad Dermatol* 31:693–708. [https://doi.org/10.1016/s0190-9622\(94\)70229-2](https://doi.org/10.1016/s0190-9622(94)70229-2).
- Berman JD. 1997. Human leishmaniasis: clinical, diagnostic, and chemotherapeutic developments in the last 10 years. *Clin Infect Dis* 24:684–703. <https://doi.org/10.1093/clind/24.4.684>.
- Bates PA. 2007. Transmission of *Leishmania* metacyclic promastigotes by phlebotomine sand flies. *Int J Parasitol* 37:1097–1106. <https://doi.org/10.1016/j.ijpara.2007.04.003>.
- Desjardins M, Descoteaux A. 1997. Inhibition of phagolysosomal biogenesis by *Leishmania* lipophosphoglycan. *J Exp Med* 185:2061–2068. <https://doi.org/10.1084/jem.185.12.2061>.
- Gueirard P, Laplante A, Rondeau C, Milon G, Desjardins M. 2008. Trafficking of *Leishmania donovani* promastigotes in non-lytic compartments in neutrophils enables the subsequent transfer of parasites to macrophages. *Cell Microbiol* 10:100–111. <https://doi.org/10.1111/j.1462-5822.2007.01018.x>.
- Lal CS, Verma RB, Verma N, Siddiqui NA, Rabidas VN, Pandey K, Singh D, Kumar S, Paswan RK, Kumari A, Sinha P, Das P. 2016. Hypertriglyceridemia: a possible diagnostic marker of disease severity in visceral leishmaniasis. *Infection* 44:39–45. <https://doi.org/10.1007/s15010-015-0811-9>.
- Liberopoulos EN, Apostolou F, Gazi IF, Kostara C, Bairaktari ET, Tselepis AD, Elisaf M. 2014. Visceral leishmaniasis is associated with marked changes in serum lipid profile. *Eur J Clin Invest* 44:719–727. <https://doi.org/10.1111/eci.12288>.
- Ghosh J, Lal CS, Pandey K, Das VNR, Das P, Roychoudhury K, Roy S. 2011. Human visceral leishmaniasis: decrease in serum cholesterol as a function of splenic parasite load. *Ann Trop Med Parasitol* 105:267–271. <https://doi.org/10.1179/136485911X12899838683566>.
- Bekaert ED, Dole E, Dubois DY, Bouma M-E, Lontie J-F, Kallel R, Malmendier CL, Ayrault-Jarrier M. 1992. Alterations in lipoprotein density classes in infantile visceral leishmaniasis: presence of apolipoprotein SAA. *Eur J Clin Invest* 22:190–199. <https://doi.org/10.1111/j.1365-2362.1992.tb01825.x>.
- Rabhi I, Rabhi S, Ben-Othman R, Rasche A, Daskalaki A, Trentin B, Piquemal D, Regnault B, Descoteaux A, Guizani-Tabbane L, Sysco Consortium. 2012. Transcriptomic signature of *Leishmania* infected mice macrophages: a metabolic point of view. *PLoS Negl Trop Dis* 6:e1763. <https://doi.org/10.1371/journal.pntd.0001763>.
- Osorio y Fortéa J, de La Llave E, Regnault B, Coppée JY, Milon G, Lang T, Prina E. 2009. Transcriptional signatures of BALB/c mouse macrophages housing multiplying *Leishmania amazonensis* amastigotes. *BMC Genomics* 10:119. <https://doi.org/10.1186/1471-2164-10-119>.
- Filippas-Ntekouan S, Liberopoulos E, Elisaf M. 2017. Lipid testing in infectious diseases: possible role in diagnosis and prognosis. *Infection* 45:575–588. <https://doi.org/10.1007/s15010-017-1022-3>.
- Ghosh J, Bose M, Roy S, Bhattacharyya SN. 2013. *Leishmania donovani* targets Dicer1 to downregulate miR-122, lower serum cholesterol and facilitate murine liver infection. *Cell Host Microbe* 13:277–288. <https://doi.org/10.1016/j.chom.2013.02.005>.
- Costa NS, Santos MO, Carvalho CPO, Assunção ML, Ferreira HS. 2017. Prevalence and factors associated with food insecurity in the context of economic crisis in Brazil. *Curr Dev Nutr* 1:e000869. <https://doi.org/10.3945/cdn.117.000869>.
- Malta DC, Andrade SC, Claro RM, Bernal RTI, Monteiro CA. 2014. Trends in prevalence of overweight and obesity in adults in 26 Brazilian state capitals and the Federal District from 2006 to 2012. *Rev Bras Epidemiol* 17:267–276. <https://doi.org/10.1590/1809-45032014000500021>.
- Ghosh J, Das S, Guha R, Ghosh D, Naskar K, Das A, Roy S. 2012. Hyperlipidemia offers protection against *Leishmania donovani* infection: role of membrane cholesterol. *J Lipid Res* 53:2560–2572. <https://doi.org/10.1194/jlr.M026914>.
- Sarnaglia GD, Covre LP, Pereira FEL, De Matos Guedes HL, Faria AMC, Dietze R, Rodrigues RR, Maioli TU, Gomes DCO. 2016. Diet-induced obesity promotes systemic inflammation and increased susceptibility to murine visceral leishmaniasis. *Parasitology* 143:1647–1655. <https://doi.org/10.1017/S003118201600127X>.
- McElrath MJ, Murray HW, Cohn ZA. 1988. The dynamics of granuloma formation in experimental visceral leishmaniasis. *J Exp Med* 167:1927–1937. <https://doi.org/10.1084/jem.167.6.1927>.
- Wilson ME, Young BM, Davidson BL, Mente KA, McGowan SE. 1998. The importance of TGF- β in murine visceral leishmaniasis. *J Immunol* 161:6148–6155.
- Wang H, Quiroga AD, Lehner R. 2013. Analysis of lipid droplets in hepatocytes. *Methods Cell Biol* 116:107–127. <https://doi.org/10.1016/B978-0-12-408051-5.00007-3>.
- Dalton JE, Glover AC, Hoodless L, Lim E-K, Beattie L, Kirby A, Kaye PM. 2015. The neurotrophic receptor Ntrk2 directs lymphoid tissue neovascularization during *Leishmania donovani* infection. *PLoS Pathog* 11:e1004681. <https://doi.org/10.1371/journal.ppat.1004681>.
- World Health Organization. 2021. Leishmaniasis. World Health Organization, Geneva, Switzerland.
- Oliveira-Lima OC, Almeida NL, Almeida-Leite CM, Carvalho-Tavares J. 2019. Mice chronically fed a high-fat diet are resistant to malaria induced by *Plasmodium berghei* ANKA. *Parasitol Res* 118:2969–2977. <https://doi.org/10.1007/s00436-019-06427-2>.
- Brima W, Eden DJ, Mehdi SF, Bravo M, Wiese MM, Stein J, Almonte V, Zhao D, Kurland I, Pessin JE, Zima T, Tanowitz HB, Weiss LM, Roth J, Nagajothi F. 2015. The bright (and evolutionarily older) face of metabolic syndrome: evidence from *Trypanosoma cruzi* infection in CD-1 mice. *Diabetes Metab Res Rev* 31:346–359. <https://doi.org/10.1002/dmrr.2636>.
- Nagajothi F, Weiss LM, Zhao D, Koba W, Jelicks LA, Cui MH, Factor SM, Scherer PE, Tanowitz HB. 2014. High fat diet modulates *Trypanosoma cruzi* infection associated myocarditis. *PLoS Negl Trop Dis* 8:e3118. <https://doi.org/10.1371/journal.pntd.0003118>.
- Lizardo K, Ayyappan JP, Cui MH, Balasubramanya R, Jelicks LA, Nagajothi JF. 2019. High fat diet aggravates cardiomyopathy in murine chronic Chagas disease. *Microbes Infect* 21:63–71. <https://doi.org/10.1016/j.micinf.2018.07.001>.
- Figueiredo VP, Lopes ES, Jr, Lopes LR, Simões NF, Penitente AR, Bearzoti E, Vieira PMDA, Schulz R, Talvani A. 2018. High fat diet modulates inflammatory parameters in the heart and liver during acute *Trypanosoma cruzi* infection. *Int Immunopharmacol* 64:192–200. <https://doi.org/10.1016/j.intimp.2018.08.036>.
- Raica M, Mogoantă L, Kondylis A, Cimpean AM. 2010. Angiogenesis in the human thymoma assessed by subclassification of tumor-associated blood vessels and endothelial cells proliferation. *Rom J Morphol Embryol* 51:627–631.
- Dea-Ayuela MA, Rama-Iñiguez S, Bolas-Fernández F. 2007. Contrasting effects of *Trichinella spiralis* and *Trichuris muris* antigens on the infection by *Leishmania infantum* in BALB/c mice. *Acta Trop* 103:212–221. <https://doi.org/10.1016/j.actatropica.2007.06.008>.
- Rousseau D, Le Fichoux Y, Stien X, Suffia I, Ferrua B, Kubar J. 1997. Progression of visceral leishmaniasis due to *Leishmania infantum* in BALB/c mice is markedly slowed by prior infection with *Trichinella spiralis*. *Infect Immun* 65:4978–4983. <https://doi.org/10.1128/iai.65.12.4978-4983.1997>.
- Hassan MF, Zhang Y, Engwerda CR, Kaye PM, Sharp H, Bickle QD. 2006. The *Schistosoma mansoni* hepatic egg granuloma provides a favorable microenvironment for sustained growth of *Leishmania donovani*. *Am J Pathol* 169:943–953. <https://doi.org/10.2353/ajpath.2006.051319>.
- Borbón TY, Scorza BM, Clay GM, Nobre de Queiroz FL, Sariol AJ, Bowen JL, Chen Y, Zhanbolat B, Parlet CP, Valadares DG, Cassel SL, Nauseef WM, Horswill AR, Sutterwala FS, Wilson ME. 2019. Coinfection with *Leishmania major* and *Staphylococcus aureus* enhances the pathologic responses to both microbes through a pathway involving IL-17A. *PLoS Negl Trop Dis* 13:e0007247. <https://doi.org/10.1371/journal.pntd.0007247>.
- Smelt SC, Engwerda CR, McCrossen M, Kaye PM. 1997. Destruction of follicular dendritic cells during chronic visceral leishmaniasis. *J Immunol* 158:3813–3821.
- Faleiro RJ, Kumar R, Hafner LM, Engwerda CR. 2014. Immune regulation during chronic visceral leishmaniasis. *PLoS Negl Trop Dis* 8:e2914. <https://doi.org/10.1371/journal.pntd.0002914>.
- Yao C, Chen Y, Sudan B, Donelson JE, Wilson ME. 2008. *Leishmania chagasi*: homogenous metacyclic promastigotes isolated by buoyant density are highly virulent in a mouse model. *Exp Parasitol* 118:129–133. <https://doi.org/10.1016/j.exppara.2007.06.012>.
- PerkinElmer Inc. 2014. Living Image software, version 4.7.3. PerkinElmer Inc, Waltham, MA.
- Weirather JL, Jeronimo SMB, Gautam S, Sundar S, Kang M, Kurtz MA, Haque R, Schriefer A, Talhari S, Carvalho EM, Donelson JE, Wilson ME. 2011. Serial quantitative PCR assay for detection, species discrimination, and quantification of *Leishmania* spp. in human samples. *J Clin Microbiol* 49:3892–3904. <https://doi.org/10.1128/JCM.00764-11>.

42. Illumina Inc. 2011. Illumina GenomeStudio 2011, version V2011.1. Illumina Inc, San Diego, CA.
43. Partek Inc. 2019. Partek Genomics Suite software, version 7.19.1125. Partek Inc, St Louis, MO.
44. Schmittgen TD, Livak KJ. 2008. Analyzing real-time PCR data by the comparative CT method. *Nat Protoc* 3:1101–1108. <https://doi.org/10.1038/nprot.2008.73>.
45. Mi H, Thomas P. 2009. PANTHER pathway: an ontology-based pathway database coupled with data analysis tools. *Methods Mol Biol* 563:123–140. https://doi.org/10.1007/978-1-60761-175-2_7.
46. Mi H, Muruganujan A, Huang X, Ebert D, Mills C, Guo X, Thomas PD. 2013. Protocol update for large-scale genome and gene function analysis with the PANTHER classification system (v.14.0). *Nat Protoc* 8:1551–1566. <https://doi.org/10.1038/nprot.2013.092>.
47. Mi H, Muruganujan A, Ebert D, Huang X, Thomas PD. 2019. PANTHER version 14: more genomes, a new PANTHER GO-slim and improvements in enrichment analysis tools. *Nucleic Acids Res* 47:D419–D426. <https://doi.org/10.1093/nar/gky1038>.
48. GraphPad Software LLC. 2020. GraphPad Prism, version 9.1.0. GraphPad Software LLC, San Diego, CA.